

# ON THE PAINLEVÉ INTEGRABILITY TO A (2+1)-DIMENSIONAL DAVEY-STEWARTSON-TYPE EQUATION: MULTIPLE SHOCK WAVE, LUMP, BREATHERS SOLUTIONS, AND OTHER PHYSICAL TRAVELING WAVE SOLUTIONS

ABDUL-MAJID WAZWAZ<sup>1,a</sup>, LAMIAA S. EL-SHERIF<sup>2,b</sup>, A. M. BAKRY<sup>2</sup>, SAMIR A. EL-TANTAWY<sup>3,4,c</sup>

<sup>1</sup>Department of Mathematics, Saint Xavier University, Chicago, IL 60655, USA

<sup>a</sup>Email: [wazwaz@sxu.edu](mailto:wazwaz@sxu.edu)

<sup>2</sup>Department of Physics, College of Science and Humanities, Prince Sattam Bin Abdulaziz University, Wadi Al-Dawaser 11991, Saudi Arabia

<sup>b</sup>Corresponding author: Email: [lamiaa\\_ph@yahoo.com](mailto:lamiaa_ph@yahoo.com)

<sup>3</sup>Department of Physics, Faculty of Science, Al-Baha University, Al-Baha P.O. Box 1988, Saudi Arabia

<sup>4</sup>Department of Physics, Faculty of Science, Port Said University, Port Said 42521, Egypt

<sup>c</sup>Email: [tantawy@sci.psu.edu.eg](mailto:tantawy@sci.psu.edu.eg)

*Compiled August 17, 2025*

In this work, we study the (2+1)-dimensional integrable Davey-Stewartson-type equation (DSE). The Painlevé analysis is applied to confirm the model's integrability. Thereafter, the Hirota bilinear method (HBM) is employed to derive the dispersion relation and phase shift, thereby exploring multiple soliton solutions. Additionally, according to HBM, both lump and breather wave solutions to the DSE are reported, with two specific examples examined for each of the two solutions. Moreover, other distinct varieties of traveling wave solutions for various physical structures are presented and studied.

*Key words:* Painlevé integrability; Hirota's bilinear method; Davey-Stewartson type equation; Multiple shock solutions; breather wave solutions; Lump solutions; Traveling wave solutions.

## 1. INTRODUCTION

Recently, there has been a surge in research studying integrable equations that appear in nonlinear science. It is well known that many physical phenomena can be described by using integrable equations. Nonlinear partial differential equations (PDEs), which describe natural phenomena in various physical contexts, have been utilized as frameworks to explain a wide range of physical phenomena in fluids, solid-state materials, oceanography, plasma waves, and many others [1–19]. To understand the interesting features of nonlinear phenomena, a series of nonlinear PDEs were formulated to describe the key characteristics of physical phenomena. The study of nonlinear evolution equations that are integrable in multiple dimensions

has constituted an intense research interest in nonlinear science. The study of nonlinear systems is essential because the solutions to these equations provide a deep understanding of the corresponding physical phenomena [20–24].

The Davey-Stewartson equation (DSE) was introduced [1, 2] to describe the evolution of a three-dimensional wave packet on water of finite depth. Maccari [2] introduced a Davey-Stewartson type equation that reads

$$u_{xt} - u_{xxxxxx} - \alpha u_{xxxy} - 5u_{xx}u_{xxx} - 5u_x u_{xxxx} - 5(u_x)^2 u_{xx} - \alpha u_x u_{xy} - \alpha u_{xx} u_y + \frac{\alpha^2}{5} u_{yy} = 0, \quad (1)$$

which can be re-written as

$$u_{xt} - u_{xxxxxx} - \alpha u_{xxxy} - 5(u_x u_{xxx})_x - \frac{5}{3}((u_x)^3)_x - \alpha(u_x u_y)_x + \frac{\alpha^2}{5} u_{yy} = 0, \quad (2)$$

where  $\alpha$  is an arbitrary constant,  $u \equiv u(x, y, t)$  is a differentiable function, and subscripts denote the corresponding derivatives. Equation (1) includes four linear terms and five nonlinear terms. In Refs. [1, 2], the integrability of the DSE equation (1) was demonstrated by using the inverse scattering method. Equation (1) describes the motion of two-dimensional water wave and has great significance in the research area of fluid mechanics [25–32].

Researchers have conducted numerous studies to explore the properties of solitons, lumps, breathers, rogue waves, and other phenomena, which have many physical applications in solitary wave theory, ocean engineering, nonlinear optics, plasmas, fluid dynamics, and shallow water waves. Solitons are stable nonlinear waves [33–38]. Lumps are rational functions and are localized in all spatial directions. A breather is a localized breathing wave with a periodic structure in a specific direction [28–37]. However, rogue waves [39–43] are localized in both space and time, appearing from nowhere and disappearing without a trace. This variety of physical solutions offers many insights into the governing wave propagation across various media. Many powerful techniques have been developed in recent decades to study nonlinear equations, including the inverse scattering transformation method [14], the modified F-expansion method, the Painlevé analysis method, the improved simple equation method [24], the Lie symmetry method [25], the generalized exponential rational function method, and many other schemes.

The organization of the paper is as follows, after the Introduction section. In Sec. 2, the new extension (1) is introduced, where its integrability is examined. We formally determine multiple soliton solutions *via* the Hirota technique in Sec. 3. Then, in Sec. 4, lump solutions are provided, and two numerical examples are examined. Breather wave solutions are explored in Sec. 5, and two numerical cases

are discussed in a manner similar to that in the previous Section. In Sec. 6, we derive a class of traveling wave solutions that encompass periodic, rational, exponential, and other types of solutions. Finally, the last Section presents some conclusions and discussion of the obtained results.

## 2. THE DAVEY-STEWARTSON-TYPE EQUATION (DSE)

Using Painlevé analysis, we will first verify whether the following DSE is integrable

$$u_{xt} - u_{xxxxxx} - \alpha u_{xxxxy} - 5u_{xx}u_{xxx} - 5u_x u_{xxxx} - 5(u_x)^2 u_{xx} - \alpha u_x u_{xy} - \alpha u_{xx} u_y + \frac{\alpha^2}{5} u_{yy} = 0. \quad (3)$$

Thereafter, we will proceed with developing the various soliton solutions for this equation, utilizing dispersion relations and phase shifts. Additional solutions featuring unique physical structures, such as lump solutions, breather wave solutions, and various traveling wave solutions, will also be shown.

### 2.1. PAINLEVÉ ANALYSIS

Numerous essential attributes, including Hamiltonian structure, the Lax pair, an infinite number of symmetries, and boundless conservation laws, can define the integrability of nonlinear evolution equations (NLEEs). We aim to investigate the Painlevé integrability of the DSE (3); therefore, we follow the Painlevé analysis technique outlined in Refs. [9–13] and related references. Weiss, Tabor, and Carnevale (WTC) [9] developed an algorithm called the WTC technique to examine the compatibility conditions for Painlevé integrability.

The equation (3) is presumed to possess a solution represented as a Laurent expansion around the manifold  $\psi \equiv \psi(x, y, t)$  as follows

$$u = \sum_{k=0}^{\infty} u_k \psi^{k-\gamma}. \quad (4)$$

The Painlevé test consists of three main steps: (i) calculating the leading-order (LO) and coefficients, (ii) identifying resonant points (RPs), and (iii) verifying compatibility conditions (CCs). Afterwards, we will examine each point in detail.

#### (i) Calculating the LO and coefficients:

The following Ansatz is considered to derive the LO behavior and coefficients

$$u = u_0 \phi^{\alpha_1}. \quad (5)$$

Now, by inserting Ansatz (5) into Eq. (3) and doing a straightforward calculation

yields:

$$\left\{ \begin{array}{l} (i) \alpha_1 = -1, u_0 = 6\phi_x, \\ (ii) \alpha_1 = -1, u_0 = 12\phi_x. \end{array} \right\} \quad (6)$$

**(ii) Determine the RPs**

Here, our objective is to identify the RPs, defined as the values of  $j$  at which arbitrary functions can be incorporated into the following Laurent series

$$u = \sum_{j=0}^{\infty} u_j \phi^{j+k}, \quad (7)$$

and it has a single value in the surroundings of the singularity manifold  $\phi$ . To accomplish this objective, we incorporate the following solution

$$u = u_0 \phi^{-1} + u_j \phi^{j-1}, \quad (8)$$

into Eq. (3), and by following the WTC analysis [5], the following two branches of RPs, namely are obtained:

(i) The principal branch (PB):  $k = -1, 1, 2, 3, 6, 10$ ,

(ii) The secondary branch (SB):  $k = -2, -1, 1, 5, 6, 12$ ,

where each branch includes six RPs due to the sixth-order of the linear structure of Eq. (3).

**(iii) Verifying CCs**

Using the methods outlined in Refs. [20–24], we can confirm the CCs. In the case of PB (i), the singular manifold  $\psi(x, y, t) = 0$  corresponds to the arbitrariness of the resonance at  $k = -1$ . We also derive explicit formulations for  $u_4, u_5, u_7, u_8$ , and  $u_9$ . Nonetheless, we discovered that  $u_1, u_2, u_3, u_6$ , and  $u_{10}$  are arbitrary functions for all non-zero real parameter values. Consequently, the (2+1)-dimensional DSE extension (3) is integrable *via* the Painlevé criterion.

For the SB (ii), the resonance at  $k = -2$  is ignored, because  $-2 < -1$ . However resonance at  $k = -1$  is explained as in case (i). We additionally derive explicit formulations for  $u_2, u_3, u_4, u_7, u_8, u_9, u_{10}$ , and  $u_{11}$ . Nonetheless, we discovered that  $u_1, u_5, u_6$ , and  $u_{12}$  are arbitrary functions for all non-zero real parameter values. Consequently, the (2+1)-dimensional DSE (3) exhibits the Painlevé integrability.

Using the obtained results of Painlevé integrability, we will pursue our work to determine multiple solitons, lump solutions, breather wave solutions, and other travelling wave solutions.

### 3. MULTIPLE SOLITON (MS) SOLUTIONS

Based on the Painlevé integrability confirmed earlier, we intend to systematically derive MS solutions for the DSE-type Eq. (3). To achieve this goal, we follow the works presented in [1–4] and some of the references therein.

Now, to find the MS solution to the integrable DSE-type Eq. (3), the following brief points are considered:

Step (I) We first consider the following Ansatz

$$u = e^{\Theta_i}, \tag{9}$$

with the phase variables  $\Theta_i = k_i x + r_i y - \omega_i t$ , where  $\omega_i$  indicate the dispersion relations (DRs), which needs to be determined.

Step (II) By substituting Ansatz (9) into Eq. (3) and resolving the resulting equations for  $\omega_i$ , we ultimately obtain

$$\omega_i = \frac{(-5k_i^6 - 5\alpha k_i^3 r_i + \alpha^2 r_i^2)}{5k_i}, \forall i = 1, 2, 3. \tag{10}$$

Step (III) Inserting the obtained values of the DRs  $\omega_i$  into the value of  $\Theta_i$ , we get

$$\Theta_i = k_i x + r_i y - \frac{(-5k_i^6 - 5\alpha k_i^3 r_i + \alpha^2 r_i^2)}{5k_i} t, \forall i = 1, 2, 3. \tag{11}$$

Step (IV) We transform Eq. (3) into its a bilinear form by using the following Hirota transformation

$$u = 6(\ln f)_x = 6\partial_x (\ln f), \tag{12}$$

where  $f \equiv f(x, y, t)$  indicates the auxiliary function (AF).

Step (V) Inserting the transformation (12) into Eq. (3) and after lengthy but straightforward calculations, we can ultimately express the Hirota bilinear form to Eq. (3) in the subsequent form

$$(D_x D_t - D_x^6 - \alpha D_x^3 D_y + \frac{\alpha^2}{5} D_y^2) f \cdot f = 0, \tag{13}$$

where  $D_t, D_x$ , and  $D_y$  indicate the Hirota derivative operators.

Equation (13) can be transformed to the following form

$$\begin{aligned} & (f f_{xt} - f_x f_t) - (f f_{xxxxx} - 6f_x f_{xxxx} + 15f_{xx} f_{xxx} - 10f_{xxx} f_{xx}) \\ & - \alpha(f f_{xxy} - 3f_x f_{xy} + 3f_{xx} f_y - f_{xxx} f_y) + \frac{\alpha^2}{5} (f f_{yy} - f_y f_y) = 0. \end{aligned} \tag{14}$$

Step (VI) We expand the AF as a perturbation series as follows:

$$f = 1 + \varepsilon f_1 + \varepsilon^2 f_2 + \varepsilon^3 f_3 + \dots, \tag{15}$$

where  $\varepsilon$  is a real and small ( $\varepsilon \ll 1$ ) parameter.

Step (VII) Now, by solving the first three-orders of  $\varepsilon$ , *i.e.*,  $O(\varepsilon)$ ,  $O(\varepsilon^2)$ , and  $O(\varepsilon^3)$  and after extensive and routine calculations, we can now determine the values of  $f_1$ ,  $f_2$ , and  $f_3$  as outlined below:

- For  $O(\varepsilon)$ , we get

$$f_1 = e^{\Theta_1}, \quad (16)$$

where  $\Theta_1$  can be obtained from Eq. (11) at  $i = 1$ .

- For  $O(\varepsilon^2)$ , we get

$$f_1 = e^{\Theta_1} + e^{\Theta_2} \text{ and } f_2 = a_{12}e^{\Theta_1+\Theta_2}, \quad (17)$$

where  $\Theta_1$  and  $\Theta_2$  can be obtained from Eq. (11) at  $i = 1$  and 2, respectively.

- For  $O(\varepsilon^3)$ , we get

$$\begin{aligned} f_1 &= e^{\Theta_1} + e^{\Theta_2} + e^{\Theta_3}, \\ f_2 &= a_{12}e^{\Theta_1+\Theta_2} + a_{23}e^{\Theta_2+\Theta_3} + a_{13}e^{\Theta_1+\Theta_3}, \\ f_3 &= A_{123}e^{\Theta_1+\Theta_2+\Theta_3}, \end{aligned} \quad (18)$$

where  $\Theta_1$ ,  $\Theta_2$ , and  $\Theta_3$  can be obtained from Eq. (11) at  $i = 1, 2$ , and 3, respectively, and  $A_{123} = a_{12}a_{23}a_{13}$ .

Step (VIII) To find the single soliton solution, the following AF is considered

$$\tilde{f}_1 = f = 1 + e^{\Theta_1}, \quad (19)$$

and by inserting Eq. (19) into Hirota transformation (12), the following single soliton solution is obtained

$$u = \frac{6k_1e^{\Theta_1}}{\tilde{f}_1}. \quad (20)$$

Step (IX) To find the two soliton solutions, the following AF is introduced

$$\tilde{f}_2 = f = 1 + e^{\Theta_1} + e^{\Theta_2} + a_{12}e^{\Theta_1+\Theta_2}, \quad (21)$$

and by inserting Eq. (21) into Hirota transformation (12), the following two soliton solutions are obtained

$$u = \frac{6}{\tilde{f}_2} (k_1e^{\Theta_1} + k_2e^{\Theta_2} + a_{12}(k_1 + k_2)e^{\Theta_1+\Theta_2}), \quad (22)$$

where  $a_{12}$  represents the phase shift between the two colliding solitons.

By substituting Eq. (21) and Hirota transformation (12) into Eq. (3), the following phase shift  $a_{12}$  is ultimately obtained

$$a_{12} = \frac{25k_1^2 k_2^2 (k_1 - k_2)^2 (k_1^2 - k_1 k_2 + k_2^2) + 5k_1 k_2 (k_1 - k_2) (k_1^2 r_2 + 2k_1 k_2 r_1 - 2k_1 k_2 r_2 - k_2^2 r_1) + \alpha^2 (k_1 r_2 - k_2 r_1)^2}{25k_1^2 k_2^2 (k_1 + k_2)^2 (k_1^2 + k_1 k_2 + k_2^2) + 5k_1 k_2 (k_1 + k_2) (k_1^2 r_2 + 2k_1 k_2 r_1 + 2k_1 k_2 r_2 + k_2^2 r_1) + \alpha^2 (k_1 r_2 - k_2 r_1)^2}. \quad (23)$$

This can be generalized as

$$a_{ij} = \frac{25k_i^2 k_j^2 (k_i - k_j)^2 (k_i^2 - k_i k_j + k_j^2) + 5k_i k_j (k_i - k_j) (k_i^2 r_j + 2k_i k_j r_i - 2k_i k_j r_j - k_j^2 r_i) + \alpha^2 (k_i r_j - k_j r_i)^2}{25k_i^2 k_j^2 (k_i + k_j)^2 (k_i^2 + k_i k_j + k_j^2) + 5k_i k_j (k_i + k_j) (k_i^2 r_j + 2k_i k_j r_i + 2k_i k_j r_j + k_j^2 r_i) + \alpha^2 (k_i r_j - k_j r_i)^2}, \quad (24)$$

for  $1 \leq i < j \leq 3$ . Because the phase shift does not vanish, this indicates that the collision between two solitons, is of inelastic collision structure. As indicated earlier, the two soliton solutions collide with phase shift  $a_{12}$  given in (23).

Step (X) To find the three soliton solutions, the following AF is introduced

$$\tilde{f}_3 = f = 1 + e^{\Theta_1} + e^{\Theta_2} + e^{\Theta_3} + a_{12} e^{\Theta_1 + \Theta_2} + a_{23} e^{\Theta_2 + \Theta_3} + a_{13} e^{\Theta_1 + \Theta_3} + A_{123} e^{\Theta_1 + \Theta_2 + \Theta_3}, \quad (25)$$

and by inserting Eq. (25) into Hirota transformation (12), the following three soliton solutions are obtained

$$u = \frac{6}{\tilde{f}_3} \left( \begin{array}{l} k_1 e^{\Theta_1} + k_2 e^{\Theta_2} + k_3 e^{\Theta_3} + a_{12} (k_1 + k_2) e^{\Theta_1 + \Theta_2} \\ + a_{13} (k_1 + k_3) e^{\Theta_1 + \Theta_3} + a_{23} (k_2 + k_3) e^{\Theta_2 + \Theta_3} \\ + A_{123} (k_1 + k_2 + k_3) e^{\Theta_1 + \Theta_2 + \Theta_3} \end{array} \right). \quad (26)$$

This result confirms the presence of three soliton solutions, thus verifying the existence of multiple soliton solutions for finite  $N$  when  $N \geq 1$ . It is worth noting that this linear relation plays a major role in deriving breather wave solutions. This fact will be observed in the coming Sections.

The profiles of one and two soliton solutions (20) and (22) are numerically examined as illustrated in Figs. 1 and 2, respectively. The numerical results demonstrate that DSE-type Eq. (3) supports shock waves instead of solitons. Figure 1 examines the single shock solution (20) as a function of the wavenumber  $k_1$ , with Fig. 1a representing  $k_1 = 0.1$  and Fig. 1b corresponding to  $k_1 = 0.15$ . Moreover, Fig. 2 examines the double shock solutions (22) as a function of the wavenumbers  $(k_1, k_2)$ , with Fig. 2a representing  $(k_1, k_2) = (0.4, 0.1)$  and Fig. 2b corresponding to  $(k_1, k_2) = (1, 0.1)$ .

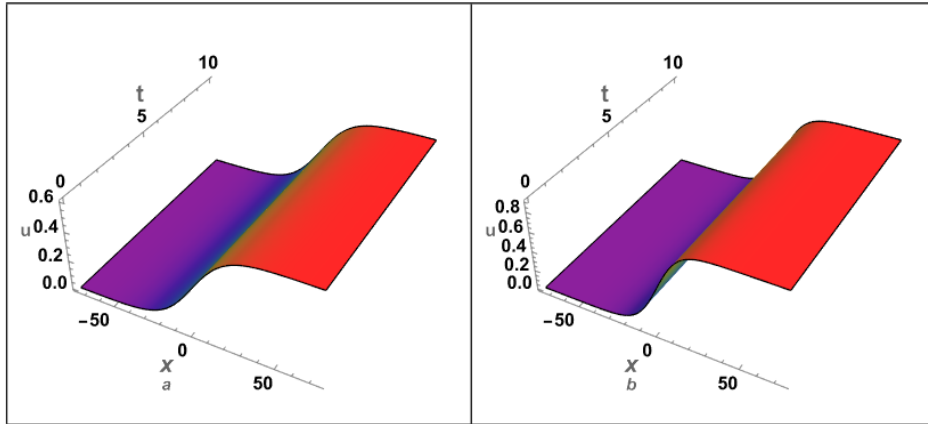


Fig. 1 – The profile of single shock wave solution (20) is plotted against  $(x, t)$ : (a) at  $k_1 = 0.1$  and (b) at  $k_1 = 0.15$ . Here,  $r_1 = 0.1$  and  $\alpha = 1$ .

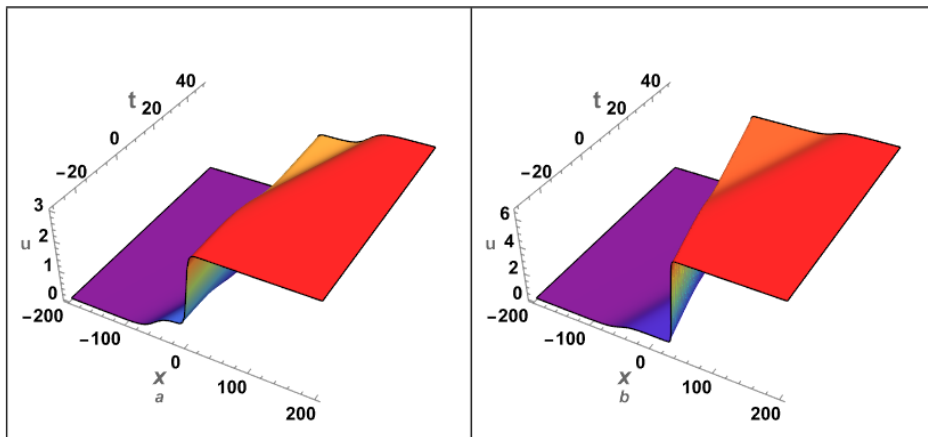


Fig. 2 – The profile of double shock wave solution (20) is plotted against  $(x, t)$ : (a) at  $(k_1, k_2) = (0.4, 0.1)$  and (b) at  $(k_1, k_2) = (1, 0.1)$ . Here,  $r_1 = 0.1$ ,  $r_2 = 0.3$ , and  $\alpha = 1$ .

#### 4. LUMP SOLUTIONS (LSS)

LSs are recognized for their localization in all spatial directions and arise from solving the integrable evolution equations. Nonetheless, soliton solutions are typically localized in both temporal and spatial dimensions, governed by exponentially localized functions [20–24]. This Section aims to derive a class of LSs for arbitrary parameter values to Eq. (3). For this purpose, Eq. (3) should be transformed into a bilinear equation as given in Eqs. (13) and (14). To obtain the lump solution for Eq. (3), the AF  $f$  must be a positive quadratic function (PQF); therefore, it is restricted to the following form to ensure its quadratic and positive qualities

$$f = (a_1x + a_2y + a_3t + a_4)^2 + (a_5x + a_6y + a_7t + a_8)^2 + a_9. \quad (27)$$

The real parameters  $a_j, 1 \leq j \leq 9$  will be formally determined. We can ascertain the values of  $a_j$  by substituting Eq. (27) into Eq. (14). Following extensive calculations, we can derive various cases for lump solutions. We provide two numerical cases as examples, acknowledging that additional cases can be identified.

**Case 1:** To determine the first set of LSs, we first consider:  $a_i = a_i, \forall i = 2, 4, 5, 8, 9$ , resulting in:

$$\left\{ \begin{array}{l} a_1 = 0, \\ a_3 = -\frac{2\alpha^3 a_2^3 a_9}{75 a_5^4}, a_5 \neq 0, \\ a_6 = \frac{\alpha a_2^2 a_9}{15 a_5^3}, \\ a_7 = -\frac{\alpha^2 a_2^2 (\alpha^2 a_2^2 a_5^2 - 225 a_5^6)}{1125 a_5^7}. \end{array} \right. \quad (28)$$

Here, it is assumed that  $a_9 > 0$  which is a necessary condition for the creation of lumps. Using Eq. (28) into Eq. (27) and Hirota transformation (12), then, the first class of LSs to Eq. (3) can be obtained as follows

$$u = \frac{6 \left[ -\frac{8}{1125} \alpha^2 (4\alpha^2 - 225)t + 2x + \frac{8}{15} \alpha y + 4 \right]}{\left( -\frac{16}{75} \alpha^3 t + 2y + 2 \right)^2 + \left[ -\frac{4}{1125} \alpha^2 (4\alpha^2 - 225)t + x + \frac{4}{15} \alpha y + 2 \right]^2 + 1}. \quad (29)$$

**Case 2:** To determine the second set of LSs, we consider:  $a_i = a_i, \forall i = 1, 2, 4, 5, 6, 8$ , resulting in:

To determine the second set of LSs, we use the next selection of parameters, resulting in:

$$\left\{ \begin{array}{l} a_3 = -\frac{\alpha^2 [a_1 (a_2^2 - a_6^2) + 2a_2 a_5 a_6]}{5(a_1^2 + a_5^2)}, \\ a_7 = -\frac{\alpha^2 [-a_5 (a_2^2 - a_6^2) + 2a_1 a_2 a_6]}{5(a_1^2 + a_5^2)}, \\ a_9 = \frac{15(a_1^2 + a_5^2)^2 (a_1 a_2 + a_5 a_6)}{\alpha (a_1 a_6 - a_2 a_5)^2}. \end{array} \right. \quad (30)$$

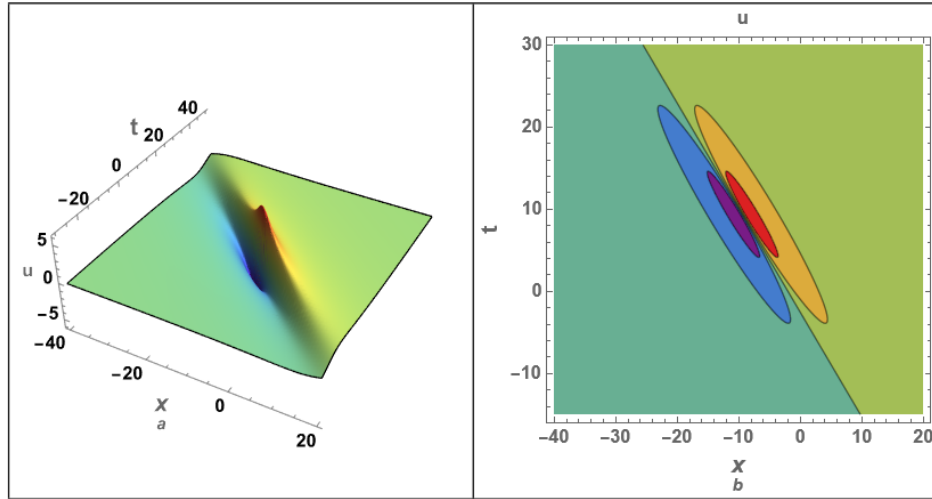


Fig. 3 – The profile of lump solution (29) is plotted against  $(x, t)$ : (a) 3D presentation for the lump solution (29) and (b) contour presentation for the lump solution (29). Here,  $\alpha = 1$ .

Here, it is assumed that  $a_9 > 0$  and  $\alpha(a_1a_6 - a_2a_5) \neq 0$ .

Also, by inserting Eq. (30) into Eq. (27) and Hirota transformation (12), we can get the second form for lump solution to problem (3).

Figure 3 represents a graphical analysis for the lump solution (29).

### 5. BREATHER WAVE SOLUTIONS (BWSS)

A breather is a nonlinear wave marked by energy concentrated in a limited, oscillatory way. The breather wave is a distinctive soliton with a periodic structure within its local region [20–26]. Breather wave solutions (BWSs) can be derived using several techniques, such as the Hirota bilinear method. This section aims to derive a class of BWSs to Eq. (3) for arbitrary parameter values. For this purpose, Eq. (3) is transformed into a bilinear equation as given by Eqs. (13) and (14). Thereafter, we established the subsequent test function as a solution

$$f = e^{-g} + c_1 e^g + c_2 \cos h, \quad (31)$$

with

$$\begin{cases} g &= a_1x + a_2y + a_3t + a_4, \\ h &= a_5x + a_6y + a_7t + a_8, \end{cases}$$

where  $c_1$  and  $c_2$  are nonzero real numbers and  $f$  must be PQF.

Here,  $a_j, \forall 1 \leq j \leq 8$  are real parameters that need to be determined. We can ascertain the values of  $a_j$  by substituting Eq. (31) into Eq. (14). Following extensive calculations using Maple or Mathematica, we can derive various cases for

lump solutions. We provide two numerical cases as examples, acknowledging that additional cases can be identified.

In what follows, we derive two sets of the parameters obtained upon using the previous analysis.

**Case 1.** Using the first set of selections of the parameters  $a_i = a_i \forall i = 1, 4, 5, 8$  and  $(c_1, c_2) = (c_1, c_2)$ , we get

$$\begin{cases} a_2 = -\frac{5a_1^3}{\alpha}, \alpha \neq 0, \\ a_3 = -9a_1^5, \\ a_6 = \frac{5a_5^3}{\alpha}, \\ a_7 = -9a_5^5, \end{cases} \quad (32)$$

which for  $(a_1, a_4, a_5, a_8) = (1, 1, 1, 2)$ , we get

$$\begin{cases} g = -9t + x - \frac{5}{\alpha}y + 1, \\ h = -9t + x + \frac{5}{\alpha}y + 2. \end{cases} \quad (33)$$

Note that the obtained values of parameters (32) generate the class of PQF solutions upon inserting Eq. (33) into Eq. (31), which leads to

$$f = e^{-(9t+x-\frac{5}{\alpha}y+1)} + c_1 e^{(-9t+x-\frac{5}{\alpha}y+1)} + c_2 \cos\left(-9t+x+\frac{5}{\alpha}y+2\right). \quad (34)$$

Thereafter, by substituting Eq. (34) into Hirota transformation (12), the following breather wave solution is obtained

$$u = \frac{6(-e^{-g} + c_1 e^g - c_2 \sin(h))}{(e^{-g} + c_1 e^g + c_2 \cos(h))}. \quad (35)$$

**Case 2.** We next use the second set of selections of the parameters, where we obtain

$$\begin{cases} a_2 = -\frac{5a_1}{\alpha} (a_1^2 - 3a_5^2), \alpha \neq 0, \\ a_3 = -9a_1 (a_1^4 - 10a_1^2 a_5^2 + 5a_5^4), \\ a_6 = -\frac{5a_5}{\alpha} (3a_1^2 - a_5^2), \\ a_7 = -9a_5 (5a_1^4 - 10a_1^2 a_5^2 + a_5^4), \end{cases} \quad (36)$$

For a numerical example, we can choose  $(a_1, a_4, a_5, a_8) = (1, 1, 1, 2)$ , which leads to

$$a_2 = \frac{10}{\alpha}, a_3 = 36, a_6 = -\frac{10}{\alpha}, a_7 = 36, \alpha \neq 0. \quad (37)$$

Accordingly, we get

$$\begin{cases} g = 36t + x + \frac{10}{\alpha}y + 1, \\ h = 36t + x - \frac{10}{\alpha}y + 2. \end{cases} \quad (38)$$

Note that obtained values of parameters (36) generate the class of PQF solutions upon inserting Eq. (38) into Eq. (31), which leads to

$$f = e^{-(36t+x+\frac{10}{\alpha}y+1)} + c_1 e^{(36t+x+\frac{10}{\alpha}y+1)} + c_2 \cos\left(36t+x-\frac{10}{\alpha}y+2\right). \quad (39)$$

Thereafter, by substituting Eq. (39) into Hirota transformation (12), the following breather wave solution is obtained

$$u = \frac{6(-e^{-g} + c_1 e^g - c_2 \sin(h))}{(e^{-g} + c_1 e^g + c_2 \cos(h))}. \quad (40)$$

Note that the obtained values of parameters (36) generate the class of PQF solutions upon inserting (32) in (31). Accordingly, a second class of BWSs to Eq. (3) can be found by inserting both Eqs. (31) and (32) into Hirota transformation (12).

The profile of the first type of breather wave solution (35) is numerically investigated as illustrated in Fig. 4.

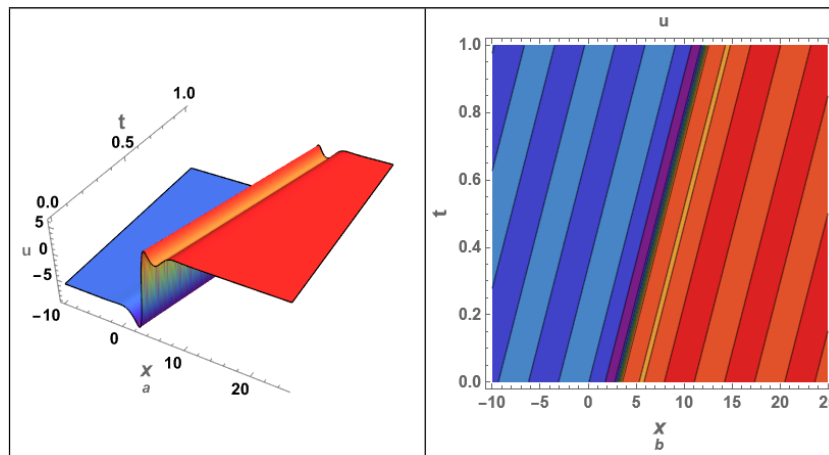


Fig. 4 – The profile of breather wave solution (35) is plotted against  $(x, t)$ : (a) 3D presentation for the breather wave solution (35) and (b) contour presentation for the breather solution (35). Here,  $\alpha = 1$ ,  $c_1 = 1$ , and  $c_2 = 2$ .

## 6. VARIETY OF OTHER SOLUTIONS

In this Section, we aim to derive additional traveling wave solutions of diverse topologies, including kink solutions, periodic single solutions, exponential solutions, and various other solution types, by employing robust methodologies [20–26].

6.1. KINK SOLUTIONS USING THE TANH TECHNIQUE

The kink solution of Eq. (3) can be generated using the tanh technique. According to this method, the solution is assumed to have the following form:

$$u = \sum_{i=0}^m a_i \tanh^i(R), \tag{41}$$

such that, by balancing higher-order nonlinearity with higher-order derivatives, the integer  $m$  can be obtained:  $m + 6 = (m + 2) + (m + 3)$ , which leads to  $m = 1$ . Note that  $R = kx + ry - wt$ . Then, relation (41) can be written as

$$u = a_0 + a_1 \tanh(kx + ry - wt), \tag{42}$$

where  $a_0$  and  $a_1$  are undetermined constants and  $w$  indicates the dispersion relation.

Now, by inserting Eq. (42) into Eq. (3), and solving the obtained result, we ultimately get

$$a_1 = 6k \text{ and } w = \frac{-80k^6 - 20\alpha k^3 r + \alpha^2 r^2}{5k}, \tag{43}$$

where  $a_0$  is a free parameter.

Using the obtained values of  $(a_1, w)$  in solution (42), the following kink solution is obtained

$$u = a_0 + 6k \tanh(R), \tag{44}$$

with

$$R = kx + ry - \left( \frac{-80k^6 - 20\alpha k^3 r + \alpha^2 r^2}{5k} \right) t. \tag{45}$$

Similarly, we can obtain the following singular solution by replacing  $\tanh(\eta)$  with  $\coth(\eta)$  in Eq. (42)

$$u = a_0 + 6k \coth(R), \tag{46}$$

where  $R$  has the same value given in Eq. (45).

6.2. PERIODIC SOLUTION USING THE TAN METHOD

Here, we can apply the tan scheme, to derive the periodic solution to Eq. (3). According to this method, we can follow the same methodology used in the tanh method to generate kink waves, which ultimately leads to:

$$u = a_0 + a_1 \tan(R), \tag{47}$$

where  $a_0$  and  $a_1$  are undetermined constants and  $w$  indicates the dispersion relation.

Now, by inserting Eq. (47) into Eq. (3), and solving the obtained result, we ultimately get

$$a_1 = -6k \text{ and } w = \frac{-80k^6 + 20\alpha k^3 r + \alpha^2 r^2}{5k}, \tag{48}$$

where other parameters have arbitrary values.

Using the obtained values of  $(a_1, w)$  in solution (47), the following periodic solution is obtained

$$u = a_0 - 6k \tan \left[ kx + ry - \left( \frac{-80k^6 + 20\alpha k^3 r + \alpha^2 r^2}{5k} \right) t \right], \quad (49)$$

with

$$R = \left[ kx + ry - \left( \frac{-80k^6 + 20\alpha k^3 r + \alpha^2 r^2}{5k} \right) t \right]. \quad (50)$$

Similarly, we can obtain the following singular solution by replacing  $\tan(\eta)$  with  $\cot(\eta)$  in Eq. (47)

$$u = a_0 + 6k \cot \left[ kx + ry - \left( \frac{-80k^6 + 20\alpha k^3 r + \alpha^2 r^2}{5k} \right) t \right], \quad (51)$$

where  $R$  has the same value given in Eq. (50).

### 6.3. RATIO OF TRIGONOMETRIC FUNCTIONS

Here, the solution to Eq. (3) is assumed to be in the following trigonometric form

$$u = \frac{\sin(R)}{a_0 + a_1 \cos(R)}, \quad (52)$$

where  $(a_0, a_1, w)$  are unknown constants that need to be determined.

We can find the values of  $(a_0, a_1, w)$  by substituting the hypothesis (52) into Eq. (3), and then solving the resulting equations to determine  $(a_0, a_1, w)$  as follows:

$$a_0 = \pm \frac{1}{3k}, a_1 = -\frac{1}{3k}, w = \frac{-5k^6 + 5\alpha k^3 r + r^2 \alpha^2}{5k}, \forall k \neq 0. \quad (53)$$

Using the obtained values of  $(a_0, a_1, w)$  in solution (52), the following trigonometric solution to Eq. (3) is obtained

$$u = \frac{\sin(R)}{\pm \frac{1}{3k} - \frac{1}{3k} \cos(R)}, \quad (54)$$

with

$$R = \left[ kx + ry - \left( \frac{-5k^6 + 5\alpha k^3 r + r^2 \alpha^2}{5k} \right) t \right]. \quad (55)$$

Similarly, we can develop a new solution in the following form

$$u = \frac{\cos(R)}{a_0 + a_1 \sin(R)}. \quad (56)$$

By applying the same methodology used in solution (54) to determine the values of  $(a_0, a_1, w)$ , we finally obtain the following values:

$$a_0 = \pm \frac{1}{3k}, a_1 = \frac{1}{3k}, w = \frac{-5k^6 + 5\alpha k^3 r + r^2 \alpha^2}{5k} \quad \forall k \neq 0. \quad (57)$$

Using the obtained values of  $(a_0, a_1, w)$  given in Eq. (57) in solution (56), the following trigonometric solution to Eq. (3) is obtained

$$u = \frac{\cos(R)}{\pm \frac{1}{3k} + \frac{1}{3k} \sin(R)}, \quad (58)$$

where  $R$  has the same value given in Eq. (55).

#### 6.4. RATIO OF HYPERBOLIC FUNCTIONS

Here, the solution to Eq. (3) is assumed to be in the following hyperbolic form

$$u = \frac{\sinh(R)}{a_0 + a_1 \cosh(R)}, \quad (59)$$

with  $R = (kx + ry - wt)$ , where  $(a_0, a_1, w)$  are unknown constants that need to be determined.

We can determine the values of  $(a_0, a_1, w)$  by inserting the hypothesis (59) into Eq. (3), and then solving the resulting equations to get the value of  $(a_0, a_1, w)$  as follows:

$$\begin{cases} a_0 = \pm \frac{1}{3k}, a_1 = \frac{1}{3k}, \\ w = \frac{-5k^6 - 5\alpha k^3 r + r^2 \alpha^2}{5k}, \forall k \neq 0. \end{cases} \quad (60)$$

Now, by inserting the obtained values of  $(a_0, a_1, w)$  into solution (59), the following hyperbolic solution to Eq. (3) is obtained

$$u = \frac{\sinh(R)}{\pm \frac{1}{3k} + \frac{1}{3k} \cosh(R)}, \quad (61)$$

with

$$R = \left[ kx + ry - \left( \frac{-5k^6 - 5\alpha k^3 r + r^2 \alpha^2}{5k} \right) t \right].$$

#### 6.5. RATIO OF EXPONENTIAL FUNCTIONS

In this Section, we discuss two different exponential form solutions for Eq. (3). According to the first form, the following solution is considered:

$$u = \frac{e^R}{a_0 + a_1 e^R}, \quad (62)$$

with the phase  $R = (kx + ry - wt)$ , where  $(a_0, a_1, w)$  are unknown constants that need to be determined.

By substituting the hypothesis (62) into Eq. (3), we can determine the values of  $(a_0, a_1, w)$  by solving the resulting equations, which leads to

$$a_1 = \frac{1}{6k} \text{ and } w = \frac{-5k^6 - 5\alpha k^3 r + r^2 \alpha^2}{5k}, \quad (63)$$

where  $a_0$  is a free parameter.

Now, by inserting the obtained values of  $(a_1, w)$  into solution (62), the following solution to Eq. (3) in the exponential form is obtained

$$u = \frac{e^R}{a_0 + \frac{1}{6k}e^R}, \quad (64)$$

with the following phase

$$R = \left[ kx + ry - \left( \frac{-5k^6 - 5\alpha k^3 r + r^2 \alpha^2}{5k} \right) t \right].$$

Furthermore, a new exponential solution to Eq. (3) can be constructed in the following form:

$$u = \frac{a_0}{1 + a_1 e^R}, \quad (65)$$

where  $(a_0, a_1, w)$  are unknown constants that need to be determined.

Now, by using the hypothesis (65) in Eq. (3), we can find the values of  $(a_0, a_1, w)$  by solving the resulting equations, which leads to

$$a_0 = -6k \text{ and } w = \frac{-5k^6 - 5\alpha k^3 r + r^2 \alpha^2}{5k}. \quad (66)$$

By substituting the obtained values of  $(a_0, w)$  given in Eq. (66) into solution (65), the following traveling wave solution to Eq. (3) is obtained

$$u = \frac{-6k}{1 + a_1 e^R}, \quad (67)$$

with the following phase

$$R = \left[ kx + ry - \left( \frac{-5k^6 - 5\alpha k^3 r + r^2 \alpha^2}{5k} \right) t \right],$$

where  $a_1$  is a non-zero free parameter.

## 7. CONCLUDING REMARKS

To summarize, this article presented an innovative analysis of the (2+1)-dimensional integrable Davey-Stewartson-type equation. The Painlevé integrability of this equation has been examined and confirmed. The efficient Hirota bilinear method

has been formally applied to derive multiple shock wave solutions for this equation. Additionally, lump wave solutions have been obtained, and two numerical examples have been analyzed. Moreover, breather wave solutions have been investigated, with two numerical examples examined. Furthermore, various distinct solutions, including kink solutions, periodic solutions, ratios of trigonometric functions, ratios of hyperbolic functions, and ratios of exponential functions, were also provided for this system. The approaches used can be applied to further studies that explore solitary wave phenomena in mathematical physics and engineering structures, significantly contributing to the field of solitary wave theory.

In future works, it is possible to solve the current equation in its fractional form and enhance one's understanding of the dynamics of the propagation of nonlinear phenomena described by it by applying various effective methodologies, such as the Tantawy technique [44–47]. This is because fractional calculus has successfully explained many physical and engineering phenomena that traditional calculus did not explain.

*Acknowledgements.* The authors extend their appreciation to Prince Sattam bin Abdulaziz University for funding this research work through the project number (PSAU/2024/01/31896).

#### REFERENCES

1. A. Davey and K. Stewartson, Proc. R. Soc. A **338**, 101-110 (1974).
2. A. Maccari, Phys. Lett. A **265**, 187-193 (2000).
3. W. Albalawi, A.-M. Wazwaz, and S. A. El-Tantawy, Rom. Rep. Phys. **77**, 109 (2025).
4. A.-M. Wazwaz, R. A. Alharbey, and S. A. El-Tantawy, Rom. Rep. Phys. **75**, 116 (2023).
5. S. M. E. Ismaeel, A.-M. Wazwaz, and S. A. El-Tantawy, Rom. Rep. Phys. **76**, 102 (2024).
6. A.-M. Wazwaz, R. A. Alharbey, and S. A. El-Tantawy, Rom. Rep. Phys. **75**, 119 (2023).
7. D. Mihalache, Rom. Rep. Phys. **76**, 402 (2024).
8. N. Liang, D. Mihalache, M. Ma, J. Rao, and Y. Liu, Rom. Rep. Phys. **76**, 106 (2024).
9. J. Weiss, M. Tabor, and G. Carnevale, J. Math. Phys. A **24**, 522-526 (1983).
10. O. I. Bogoyavlenskii, Russ. Math. Surv. **45**, 1 (1990).
11. J. Schiff, *Painlevé Transcendents: Their Asymptotics and Physical Applications*, Plenum, New York (1992).
12. C. M. Khalique and A. Anila Mehmood, Results in Physics **25**, 104194 (2021).
13. A.-M. Wazwaz, Appl. Math. Comput. **217**(8), 4282-4288 (2010).
14. B. A. Malomed and D. Mihalache, Rom. J. Phys. **64**, 106 (2019).
15. K. L. Tian, G. M. Lai, G. Yi, and Y. Xu, Rom. Rep. Phys. **76**, 103 (2024).
16. A.-M. Wazwaz, Rom. Rep. Phys. **76**, 114 (2024).
17. Zhou-Zheng Kang, Rom. J. Phys. **69**, 109 (2024).
18. Jin-Yun Yang and Wen-Xiu Ma, Rom. J. Phys. **69**, 101 (2024).
19. Xiaolin Yang, Yi Zhang, and Wenjing Li, Rom. J. Phys. **69**, 102 (2024).
20. R. Hirota, *The Direct Method in Soliton Theory*, Cambridge University Press, Cambridge (2004).

21. C. M. Khalique and K. A. Maefo, *Mathematical Biosciences and Engineering* **18**(5), 5816-5835 (2021).
22. T. Motsepa and C. M. Khalique, *Adv. Math. Models Appl.* **5**, 7-18 (2020).
23. S. Salem, M. Kassem, and S. M. Mabrouk, *Am. J. Appl. Math.* **7**, 137-144 (2019).
24. D. Mihalache, *Rom. Rep. Phys.* **69**, 403 (2017).
25. Q. Xing, Z. Wu, D. Mihalache, and J. He, *Nonlinear Dyn.* **89**, 2299-2310 (2017).
26. G. Q. Xu, *Applied Mathematics and Computation* **217**, 5967-5971 (2011).
27. Q. Zhou and Q. Zhu, *Waves in Random and Complex Media* **25**(1), 52-59 (2014).
28. S.-L. Xu, Q. Zhou, D. Zhao, M. R. Belic, and Y. Zhao, *Appl. Math. Lett.* **106**, 106230 (2020).
29. S. A. Khuri, *Chaos, Solitons and Fractals* **26**, 25-32 (2005).
30. S. A. Khuri, *Chaos, Solitons and Fractals* **36**, 1181-1188 (2008).
31. S. A. Khuri, *Phys. Lett. A* **395**, 127218 (2021).
32. P. J. Olver, *J. Math. Phys.* **18**(6), 1212-1215 (1977).
33. Y. S. Özkan, E. Yaşar, and C. M. Khalique, *Journal of Computational Science* **73**, 102144 (2023).
34. O. D. Adeyemo and C. M. Khalique, *Alexandria Engineering Journal* **73**, 751-769 (2023).
35. C. M. Khalique and M. Y. T. Lephoko, *Open Physics* **21**(1), 0230103 (2023).
36. H. Wang, Q. Zhou, and W. Liu, *Journal of Advanced Research* **38**, 179-190 (2022).
37. G. Xu, Y. Liu, and W. Cui, *Appl. Math. Lett.* **132**, 108184 (2022).
38. N. Raza, S. Arshed, and A.-M. Wazwaz, *Phys. Lett. A* **458**, 128589 (2023).
39. S. A. El-Tantawy and A.-M. Wazwaz, *Phys. Plasmas* **25**, 092105 (2018).
40. S. A. El-Tantawy, A. H Salas, Haifa A. Alyousef, and M. R. Alharthi, *Chaos, Solitons and Fractals* **1635**, 112612 (2022).
41. S. A. El-Tantawy, A.-M. Wazwaz, and R. Schlickeiser, *Control. Fusion* **57**, 125012 (2015).
42. S. A. El-Tantawy, A.-M. Wazwaz, and S. Ali Shan, *Phys. Plasmas* **24**, 022105 (2017).
43. S. A. El-Tantawy, A.-M. Wazwaz, and Ata-ur Rahman, *Phys. Plasmas* **24**, 022126 (2017).
44. S. A. El-Tantawy, S. I.H. Bacha, M. Khalid, and W. Alhejaili, *Braz. J. Phys.* **55**, 123 (2025).
45. S. A. El-Tantawy, W. Alhejaili, M. Khalid, and A. S. Al-Johani, *Braz. J. Phys.* **55**, 176 (2025).
46. S. A. El-Tantawy, D. Khan, W. Khan, M. Khalid, and W. Alhejaili, *Braz. J. Phys.* **55**, 163 (2025).
47. S. A. El-Tantawy, M. Khalid, S. I. H. Bacha, Haifa A. Alyousef, and L. S. El-Sherif, *Braz. J. Phys.* **55**, 191 (2025).